Co-published by
Institute of Fluid-Flow Machinery
Polish Academy of Sciences
Committee on Thermodynamics and Combustion
Polish Academy of Sciences

http://www.imp.gda.pl/archives-of-thermodynamics/

Exergetic performance coefficient analysis of direct methanol fuel cell

Xinjia Guo[a], Zhanghao Lu[b], Zheshu Ma[a*], Hanling Song[a], Yuting Wang[a]

[a]College of Automobile and Traffic Engineering, Nanjing Forestry University, Nanjing, 210037, China
[b]School of Mechanical and Automobile Engineering, Jinken College of Technology, Nanjing, 211156, China
*Corresponding author email: mazheshu@njfu.edu.cn

Received: 27.10.2023; revised: 17.02.2024; accepted: 10.03.2024

Abstract

In order to improve the output performance of direct methanol fuel cell, the finite-time thermodynamic model of direct methanol fuel cell is developed in this paper. Then, mathematical expressions for energy efficiency, power density, exergy efficiency and exergy coefficient of performance are derived. In addition, the effects of operating temperature, inlet pressure and membrane thickness on the performance of direct methanol fuel cells are considered. The results show that the exergetic performance coefficient not only considers the exergy loss rate to minimize the loss, but also the power density of the direct methanol fuel cell to maximize its power density and improve its efficiency. Therefore, the exergetic performance coefficient is a better performance criterion than conventional power and efficiency. In addition, increasing the inlet pressure and decreasing the membrane thickness can significantly improve the exergetic performance coefficient and energy efficiency.

Keywords: Direct methanol fuel cell; Exergy analysis; Exergetic performance coefficient

Vol. 45(2024), No. 3, 185–195; doi: 10.24425/ather.2024.151230

Cite this manuscript as: Guo, X., Lu, Z., Ma, Z., Song, H., & Wang, Y. (2024). Exergetic performance coefficient analysis of direct methanol fuel cell. *Archives of Thermodynamics*, 45(3), 185–195.

1. Introduction

Liquid methanol is considered to be a suitable fuel for fuel cell vehicles due to its high energy density, easier storage, and the fact that it can continue to be used in conventional fuel tanks when applied to vehicles. Methanol is very stable as a fuel, has low volatility and remains liquid over a range of temperatures. As a result, direct methanol fuel cells (DMFCs) are widely used in small portable devices (e.g. laptops and portable power supplies) [1,2] and large installations (e.g. vehicles and stationary power generation equipment) [3,4].

Currently, DMFC research consists mainly of performance testing of internal components such as membranes and catalysts. Yildirim et al. [5] prepared sulfonated poly(phthalazinone ether ketone) impregnated microporous membrane – into a polyethylene support (SPPEK-PE) and pure SPPEK membrane, set different methanol concentrations and conducted experiments in order to analyze the effect of different polymer membrane impregnation on the performance of DMFC fuel cell. The experimental results showed that SPPEK-PE enhanced the performance of DMFC. Li et al. [6] synthesized a novel bifunctional polyhedral oligomeric silsesquioxane (POSS) with vinyl and su-

Nomenclature

A – effective area of the electrode, m^2
A_L – corresponding thermal leakage area,m^2
C_p – constant specific heat of the gas, constant
E_{nernst} – reversible potential, V
e_n^{ch} – chemical exergetic energy of each component, kJ/kg
ex – exergy, kJ/kg
ex_{rw} – recoverable residual exergy, kJ/kg
ex_{uw} – non-recoverable residual exergy, kJ/kg
F – Faraday
f_{exd} – exergy destruction factor
$G_{f,liq}$ – liquid Gibbs function, J
ΔH – total energy absorbed from methanol and oxygen, J
Δh – change in standard molar enthalpy, kJ/kg
K_L – thermal leakage coefficient
k – specific heat rate, J/(kg·K)
j – current density, A/m^2
j_0 – exchange current density, A/m^2
j_1 – limiting current density, A/m^2
n – number of electron transfers
P – power density of DMFC, W/m^2
$\overline{P}$ – maximum output power density of DMFC, W/m^2
P_{max} – maximum output power density of DMFC at operating temperatures, W/m^2
$P_{1,max}$ – maximum power density of DMFC at operating pressure p = 1 atm, W/m^2
p_0 – standard pressure, atm
Q_H – remaining component of the thermal rate of DMFC, J
Q_L – thermal leakage rate from DMFC to the environment, J
R – equivalent resistance caused by the three overpotentials, Ω
R_{ohm} – operating temperature of DMFC, K
r_{rw} – recoverable residual exergy ratio
r_{uw} – non-recoverable residual exergy ratio
T – temperature of the DMFC, K
T_0 – temperature of the environment, K
t_{mem} – thickness of the membrane, cm
V – voltage, V
x_n – molar fraction of the components

Greek symbols

α – transfer coefficient
β – magnification constant
η – output efficiency

Subscripts and Superscripts

act – activation overpotential
CO_2 – carbon dioxide
cell – fuel cell
ch – chemical
conc – concentration overpotential
H – hydrogen
H_2O – water
in – inlet
meoh – methanol
n – number
O_2 – oxygen
ohm – ohmic overpotential
out – outlet
ph – physical
rw – recoverable residual exergy
uw – non-recoverable residual exergy

Abbreviations and Acronyms

DMFC – direct methanol fuel cell
ECOP – ecological coefficient of performance
EDI – environmental destruction index
EPC – exergetic performance coefficient
POSS – polyhedral oligomeric silsesquioxane
SPPEK – sulfonated poly(phthalazinone ether ketone)

lfonic groups (Vi-POSS-SO_3Na) and crosslinked it by a simple in situ heat treatment, which significantly improved the properties of this proton exchange membrane. Huang et al. [7] used sulfonated spunlace carbon as a filler for SPEEK membranes, and the synthesized membranes showed improved performance as DMFC. The results showed that the MOF-C-SO3H@SPEEK membrane has good ionic conductivity compared to Nafion 115, and its special structure helps to reduce methanol penetration from the anode to the cathode, and promotes the speed of protons across the membrane. Yogarathinam et al. [8] embedded proton membrane (SPEEK) of DMFC with (PANI-A-BN). The results showed that the water absorption (58.42 %) and ionic conductivity of the PANI-A-BN/SPEEK membrane could be significantly enhanced. The methanol permeability of BN and functionalized BN embedded in SPEEK nanocomposite membranes was significantly reduced.

Currently, the methanol single cell is studied in a large number of theoretical and experimental studies. Yuan et al. [9] achieved a reduction in methanol volatility and methanol permeation using capillary distillation. Experiments were then designed to demonstrate the reduction of the relative volatility of methanol/water by the selected carbon aerogel. The results show that by providing a suitable methanol/water ratio in the vapor supply to DMFC, methanol permeation and water deficiency can be significantly mitigated, resulting in DMFC that exhibits excellent performance and stability. Mathew et al. [10] designed, fabricated and tested DMFC stacks with an effective area of 16 cm^2 and experimentally investigated the effect of various operating parameters on the performance of DMFC stacks. The results show that increasing battery temperature, cathode flow rate and methanol concentration can improve the performance of DMFC. Li et al. [11] developed an energy analysis model for direct methanol fuel cells and derived expressions for electrical, thermal and total energy efficiencies. Hotz et al. [12] performed a numerical analysis of the energy efficiency of direct methanol fuel cells, showing the importance of exergy analysis of the fuel cell as part of the overall thermal system for power generation. Yang et al. [13] developed a semi-empirical model of a direct methanol fuel cell and experimentally investigated the performance of four operating parameters, such as temperature and methanol concentration, under different operating conditions. Liu et al. [14] developed a finite-time thermodynamic model of PEMFC, including exergy efficiency and ECOP. The findings show that the heat loss of components such as functioning fuel cells is the most serious. At low current densities, the ecological performance and economy of the fuel cell system is

better, while at high current densities, the exergy loss and net power of the system increases. Li et al. [15] proposed an ecological performance factor and an ecological objective function, which are defined as the ratio of power to power loss and the difference between power and power loss. In the above study, the aspect of exergy analysis to get the performance metrics of DMFC under various operating conditions and using the performance metrics to define the output performance of DMFC is still not enough.

In recent years, finite-time thermodynamics (FTT) has been used to criticize various kinds of thermodynamic processes and cycles. Chen et al. [16] applied finite-time thermodynamics for exergy analysis in a solar thermal power system and found that the system had a positive impact on both energy and exergy performance. Qi et al. [17] developed a finite-time thermodynamic model of a two-stage multivariable temperature difference generator, considered losses such as external heat transfer and collector radiation losses, and studied the basic performance of the system. The results showed that the system performance is optimal when the external heat transfer form and internal structure parameters are optimized. Qi et al. [18] developed a thermo-Brownian heat engine model based on finite-time thermodynamics, and numerically investigated the heat transfer process and the influence of important parameters on the output performance of the system. The results showed that enhanced heat transfer can improve the performance of the system.

The electrochemical model of DMFC can be modeled as finite-time thermodynamic model through exergy analysis, which can be used for thermodynamic performance study [19,20] and optimization to get the best performance [21]. Currently, typical optimal finite-time thermodynamic objective functions include exergy loss, exergy efficiency, ecological coefficient of performance [22], ecological function [23], and entropy yield. Akkaya et al. [24] defined the coefficient of exergy performance (EPC) for analyzing the performance of solid oxide fuel cell. EPC is a thermal-ecological indicator that combines energy and hydronium parameter functions. Therefore, EPC allows for a better evaluation of thermodynamic processes and cycles that include DMFC than traditional performance metrics such as power and efficiency.

In this paper, finite-time thermodynamics is introduced to analyze the irreversibility of DMFC, and a mathematical model of DMFC considering irreversible loss is established, which not only explored the thermodynamic performance of DMFC under different parameters, better defined the source of polarization loss of the fuel cell and provided a direction for the improvement of the performance of the fuel cell, but the result obtained can also provide some kinds of theoretical instructions for the optimized design and practical usage of fuel cell.

2. Theory and methodology

2.1. Working principle of DMFC

DMFC consists of an electrode plate, catalyst layer, diffusion layer, proton exchange membrane, diffusion layer and electrolyte, and its working principle is as follow [25,26] (Fig. 1): during its operation, CH_3OH is continuously transported to the anode chamber, where it reacts with H_2O to form CO_2, H^+ and e^- with the assistance of the anode catalyst, and the generated CO_2 is discharged from the outlet of the anode chamber. H^+ reaches the cathode chamber through the proton exchange membrane and converges with e^- and O_2 transferred from the external circuit to produce H_2O, which is discharged from the outlet of the cathode chamber.

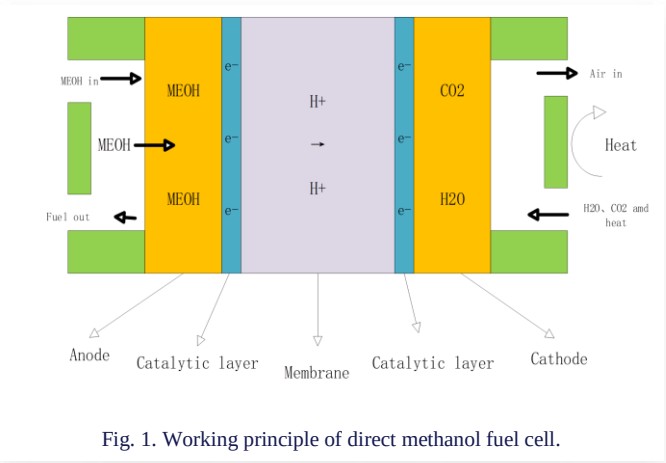

Fig. 1. Working principle of direct methanol fuel cell.

The electrochemical reaction equations of DMFC are:

- Anode:

$$CH_3OH + H_2O \rightarrow CO_2 + 6H^+ + 6e^-, \quad (1)$$

- Cathode:

$$\frac{3}{2}O_2 + 6H^+ + 6e^- \rightarrow 3H_2O, \quad (2)$$

- Over reaction:

$$CH_3OH + \frac{3}{2}O_2 \rightarrow CO_2 + 2H_2O. \quad (3)$$

The main assumptions cited in the DMFC system model are as follows:

1. DMFC system is working in steady state.
2. All types of gases in DMFC are ideally compressible, with air consisting of 21% oxygen and 79% nitrogen.
3. Only physical and chemical exergy is considered, no potential exergy and kinetic exergy are considered.
4. The distribution characteristics of the temperature of the electric stack are not considered.
5. The operating temperature of the stack is uniform.

For DMFC, the reversible potential can be given by the equation [27]:

$$E_{nernst} = -\frac{G_{f,liq}}{nF} + \frac{RT}{nF} + \ln\left[\frac{P_{meoh}\left(P_{O_2}^{\frac{3}{2}}\right)}{P_{CO_2}\left(P_{H_2O}\right)^2}\right]. \quad (4)$$

In Eq. (4), $G_{f,liq}$ is the liquid Gibbs function; n is the number of electron transfers; F is the Faraday constant; T is the operating temperature of DMFC; R is the gas constant.

2.2. Overpotential of DMFC

Polarization can have a significant impact on the performance of DMFC. The causes of polarization phenomena include polar-

ization caused by the electrochemical reaction rate of the active substances at the positive and negative electrodes being less than the rate of electron movement, and polarization caused by the depletion of reactants that cannot be replenished in time at the electrode surface. This means that some energy will be consumed to overcome this resistance during DMFC operation. In general, the polarization phenomenon produces three types of overpotentials: activation overpotential, ohmic overpotential, and concentration overpotential.

The electrochemical reaction rate of DMFC affects the activation overpotential. When the electrochemical reaction rate of positive and negative active substances is less than the rate of electron movement, the polarization loss is more serious, the loss generated by activated polarization increases, and the activation overpotential increases. In addition, the higher the activity of the catalyst used for the cathode and anode, the lower the activation loss generated, and the activation overpotential will be reduced accordingly. The activation overpotential V_{act} can be expressed as follows [27]:

$$V_{act} = \frac{RT}{\alpha nF} \log \frac{j}{j_0}, \tag{5}$$

where α is the transfer coefficient and j_0 is the exchange current density.

Ohmic polarization is polarization due to the contact resistance that exists between the electrolyte, the electrode material, the diaphragm resistance and the various component parts. For DMFCs, the ohmic resistance consists of two main components: the resistance of the ions as they cross the proton exchange membrane and the resistance of the electrons as they reach the end of the electrode. The ohmic overpotential V_{ohm} can be expressed as follows [27]:

$$V_{ohm} = jR_{ohm}, \tag{6}$$

$$R_{ohm} = \int_0^{t_{mem}} \frac{dt_{mem}}{0.04107 + 0.01878e^{100t_{mem}}}, \tag{7}$$

where R_{ohm} is the equivalent resistance caused by the three overpotentials, l_{mem} is the thickness of the membrane.

In the working process of DMFC, concentration polarization occurs when the electrode surface is not replenished in time because the reactants are consumed too quickly, and the electrode reaction surface is unable to maintain the concentration of the reaction gas as it should be. The expression for the concentration overpotential V_{conc} is as follows [27]:

$$V_{conc} = \left(1 + \frac{1}{\beta}\right) \frac{RT}{nF} \ln\left(1 - \frac{j}{j_1}\right), \tag{8}$$

where β is the magnification constant and j_1 is the limiting current density.

The irreversible output voltage V_{cell} of the DMFC can be expressed as:

$$V_{cell} = E_{nernst} - V_{act} - V_{conc} - V_{ohm} = -\frac{G_{f,liq}}{nF} + \frac{RT}{nF} + \ln\left[\frac{P_{meoh}\left(P_{O_2}^{\frac{3}{2}}\right)}{P_{CO_2}\left(P_{H_2O}\right)^2}\right] - \frac{RT}{\alpha nF} \lg \frac{j}{j_0} - jR_{ohm} - \left(1 + \frac{1}{\beta}\right) \frac{RT}{nF} \ln\left(1 - \frac{j}{j_1}\right). \tag{9}$$

The power density of DMFC can be expressed as:

$$P = V_{cell}\, jA, \tag{10}$$

where j is the current density and A is the effective area of the electrode.

As an energy conversion device, the output efficiency of DMFC can be shown in Eq. (7) [23]:

$$\eta = -\frac{P}{\Delta H}, \tag{11}$$

where ΔH is the total energy absorbed from methanol and oxygen, which can be expressed as [22]:

$$\Delta H = -\frac{jA\Delta h}{nF}, \tag{12}$$

where Δh is the change in standard molar enthalpy.

The thermal leakage rate from DMFC to the environment can be expressed as [28]:

$$Q_L = K_L A_L (T - T_0), \tag{13}$$

where K_L and A_L represent the thermal leakage coefficient and the corresponding thermal leakage area, respectively. T_0 is the temperature of the environment.

Following the first law of thermodynamics, the remaining component of the thermal rate of DMFC can be expressed as:

$$Q_H = -\Delta H - P - Q_L = \frac{A}{nF}[-(1-\eta)j\Delta h - b_1(T - T_0)], \tag{14}$$

where, $b_1 = \frac{nFK_LA_L}{A}$ [28].

2.3. Exergetic performance analysis of DMFC

The output performance of DMFC is reduced due to different irreversible loss, including heat loss, gas-flow channel friction loss, leakage current and polarization loss. Exergy analysis evaluates the actual useful fraction of energy and can therefore be used as a measure of the quality of the energy released by the DMFC. The exergy balance of DMFC is show in Fig. 2.

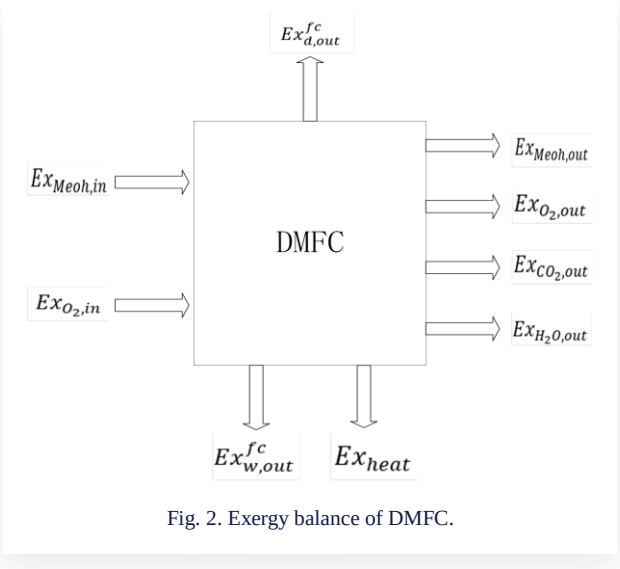

Fig. 2. Exergy balance of DMFC.

In the reaction process of DMFC, only physical and chemical exergy are considered [29,30]. The expressions of physical and chemical exergy are as follows [31,32]:

$$(ex)^{ph}=C_pT_0\left[\frac{T}{T_0}-1-\ln\left(\frac{T}{T_0}\right)+\ln\left(\frac{p}{p_0}\right)^{\frac{k-1}{k}}\right], \quad (15)$$

$$(ex)^{ph}=\sum x_n e_n^{ch}+RT_0\sum x_n \ln x_n, \quad (16)$$

where C_p is the constant specific heat of the gas, p_0 is the standard pressure, K is the specific heat rate, x_n is the molar fraction of the components and e_n^{ch} is the chemical exergetic energy of each component.

In DMFC, the total input exergy and output exergy are shown as follows:

$$ex_{in}=-\frac{jA}{nF}\left(ex_{meoh}+\frac{3}{2}ex_{O_2}\right), \quad (17)$$

$$ex_{out}=-\frac{jA}{nF}\left(2ex_{H_2O}+ex_{CO_2}\right). \quad (18)$$

In practice, the quality of energy decreases during transfer processes, including friction, drag, radiation and heat transfer. Exergy loss can be used to express the degree of irreversibility of the energy transfer process. For DMFC, the lower the exergy loss in the thermodynamic process, the higher the effective utilization of energy [32]:

$$ExD=ex_{in}-ex_{out}-P-Q_H\left(1-\frac{T}{T_0}\right). \quad (19)$$

The recoverable residual exergy ratio can be assumed to be the ratio of the recoverable residual exergy of the DMFC to the total exergy input. The recoverable residual exergy ratio can be expressed as:

$$r_{rw}=\frac{ex_{rw}}{ex_{in}}. \quad (20)$$

The non-recoverable residual exergy ratio includes the physical consumption of unused methanol and unused oxygen and heat, as well as the logistical exergy to generate water. The ratio of non-recoverable residual energy can be expressed as:

$$r_{uw}=\frac{ex_{uw}}{ex_{in}}. \quad (21)$$

In the above equation, ex_{rw} and ex_{uw} can be calculated by the following equations, respectively:

$$ex_{uw}=\dot{m}_{Meoh,out}\times ex_{Meoh,out}^{ch}+\dot{m}_{O_2,out}\times ex_{O_2,out}^{ch}, \quad (22)$$

$$ex_{rw}=\dot{m}_{Meoh,out}\times ex_{Meoh,out}^{ph}+\dot{m}_{O_2,out}\times ex_{O_2,out}^{ph}+$$
$$+\dot{m}_{HO_2,out}\times ex_{HO_2}+Ex_Q. \quad (23)$$

The exergy destruction factor is an important parameter of DMFC that indicates the impact of DMFC on exergy sustainability.exergy destruction factor can be expressed as:

$$f_{exd}=\frac{ExD}{ex_{in}}. \quad (24)$$

The environmental destruction index is used to indicate the residual exergy output that cannot be recovered from DMFC operation and the environmental impact caused by exergy destruction. This coefficient rises with the decrease of exergy efficiency. Therefore, for the practical application of DMFC, EDI should be fully considered, and appropriate operating and design conditions should be selected. The optimal reference value of "1" for EDI indicates the reversibility of exergy efficiency, where the residual exergy that cannot be recycled is close to zero. EDI is a function of *ExD*, the non-recyclable residual exergy ratio and the environmental damage factor and can be expressed as:

$$\mathrm{EDI}=(r_{uw}+f_{exd})\frac{ex_{in}}{P}=\frac{ex_{uw}-ExD}{ExD}. \quad (25)$$

In DMFC systems, energy analysis can analyze and study the processes of energy flow, conversion and storage in the system, while exergy performance analysis can visually grasp the impact of irreversible loss in the system on DMFC. Based on ecological and DMFC performance considerations, the performance of DMFC is evaluated by combining both energy and energy performance aspects, and the evaluation indicator is defined as an alternative criterion, which is more accurate and practical, and can be expressed as:

$$\mathrm{EPC}=\frac{P}{ExD}=\frac{E_{cell}jA}{ex_{in}-ex_{out}-P-Q_H\left(1-\frac{T}{T_0}\right)}. \quad (26)$$

2.4. Comparison of different objective functions

There are dimensional and order-of-magnitude differences between the indicators, therefore, in order to visualize the relationship between EPC, *P*, η and *ExD* more conveniently and intuitively, this paper uses a dimensionless method for numerical study and analysis. The dimensionless functions of EPC, *P*, η and *ExD* are expressed as EPC = EPC/EPC$_{max}$, $P = P/P_{max}$, $ExD = ExD/ExD_{max}$, $\eta = \eta_{ex}/\eta_{ex_{max}}$, $\eta = \eta/\eta_{max}$.

The dimensionless maximum output power density of DMFC can be expressed as follows:

$$\bar{P}=\frac{P_{max}}{P_{1,max}}, \quad (27)$$

where P_{max} is the maximum output power density of DMFC at different operating temperatures, and $P_{1,max}$ is the maximum power density of DMFC at operating pressure p = 1 atm. The dimensionless methods of output efficiency, exergy efficiency and exergy performance coefficient corresponding to the maximum power density are similar to the dimensionless maximum power density.

3. Results and discussion

In existing systems for evaluating DMFC performance, power and efficiency are commonly used. However, power and efficiency are only evaluated from the perspective of mechanical, friction loss to the performance of DMFC. Heat loss is also a very important phenomenon in practical applications. DMFC generates a large amount of heat loss during operation, so heat dissipation needs to be taken into account when evaluating its performance. EPC is defined as the ratio of power to heat dissi-

pation, taking into account both mechanical and heat loss. The conclusions obtained when evaluating the performance of DMFC using EPC will be more realistic and accurate.

The relevant parameters in the DMFC model are shown in Table 1. According to the input parameters, the thermodynamic irreversibility and exergy performance coefficients of DMFC with different operating parameters were investigated.

Table 1. Relevant data of DMFC.

Parameter	Value
Current Density, I (Am^{-2})	0-20000
Faraday Constant, F ($Cmol^{-1}$)	96485
Gas Constant, R ($Jmol^{-1}K^{-1}$)	8.314
Number of electrons, n	6
Ambient Temperature, T (K)	298.15
Anode Pressure (atm)	1 [33]
Cathode Pressure (atm)	1 [33]
Anode Gas Compositions	100 % MEOH [33]
Cathode Gas Compositions	21 % O_2; 79 % N_2 [33]
Transfer coefficient, α	0.3 [33]
Active area, A (cm^{-2})	25 [33]

Figure 3 compares the predicted model potential and experimental data of DMFC at 333–353 K (p = 1 atm; l_{mem} = 0.02 mm). From the experimental results in Fig. 3, it can be seen that the error between the predicted data and the experimental data is about 11%. This experimental result shows that the model has good accuracy. The relationship between polarization loss potential, output voltage and current density is shown in Fig. 3.

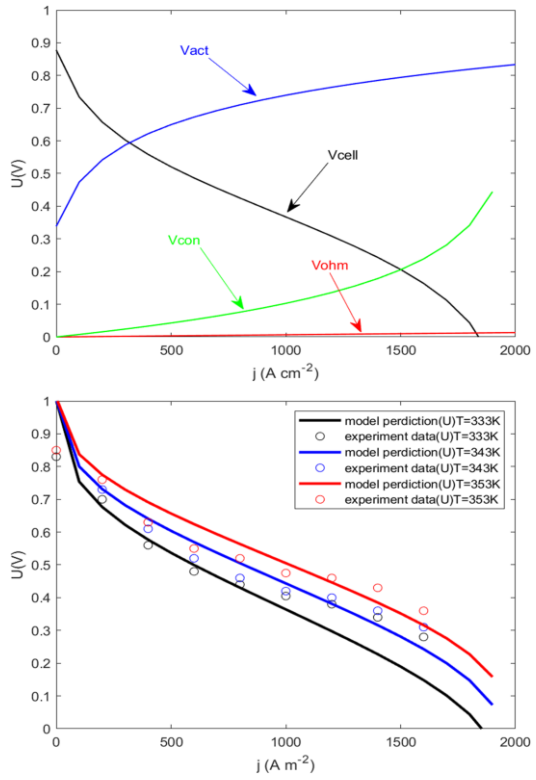

Fig. 3. Comparison of predicted model voltage and power density with experimental data[30].

As shown in Fig. 3, all three overpotentials increase with increasing current density, where the concentration overpotential increases exponentially, the activation overpotential increases logarithmically, and the ohmic overpotential increases by a small amount. When in the lower current density region, the activation overpotential rises sharply in this region, and activation loss dominates in this phase. In the medium to high current density part, the increase in concentration overpotential is larger, and in this stage, the concentration overpotential has a greater effect on the voltage variation.

3.1. Comparsion of relationship between EPC, *P*, *ExD* and *η*

As can be seen in Fig. 4, when the EPC reaches its maximum value, the efficiency is 0.41, $\eta_{ex}/\eta_{ex_{max}}$ is 1, and P/P_{max} is 0.55. This means that the power density under the EPC is very close to the maximum value. When P is at its maximum value, the efficiency is 0.24, $\eta_{ex}/\eta_{ex_{max}}$ is 0.34, and $\mathrm{EPC}/\mathrm{EPC}_{max}$ is 0.57. Obviously, compared with P_{max}, if EPC_{max} is used as the standard, the efficiency of the breakdown is improved by 66%, the breakdown loss is reduced by 70%, the efficiency is improved by 41%, and the power density is reduced by 45%. Therefore, this paper derives EPC , which takes into account not only the exergy loss to minimize the loss but also the power density of DMFC to maximize the power and improve its output performance.

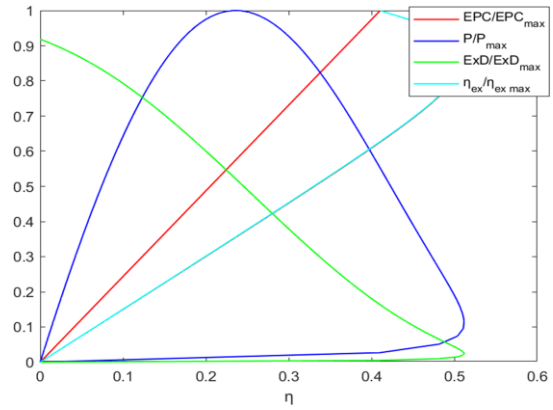

Fig. 4. The relationship between η and dimensionless EPC, P, η_{ex}.

It can be seen from Fig. 5 that the working temperature has a very obvious effect on the output performance of DMFC, which is mainly due to the fact that when the working temperature increases, the activity of the cathode and anode catalysts is enhanced, which improves the electrochemical reaction rate of the positive and negative active substances; the diffusion coefficient of the reacting gases is increased, and the internal mass transfer conditions are improved. Both $\overline{P}$ and $\overline{\mathrm{EPC}}$ of DMFC increase with the increase of operating temperature, and in the low current density region, the performance improvement brought by increasing temperature is much smaller than that in the high current density region. This is mainly due to the reason that in the low current density region, the electrochemical reaction has just started, the electrochemical reaction rate is low, and the op-

erating temperature has little effect on the electron and proton activity, so increasing the operating temperature has little effect on the electrochemical reaction rate, and only increasing the current density can accelerate the electrochemical reaction rate. Then, the irreversible loss of DMFC is dominated by activation loss in the low current density region, while the increase of activation loss in the high current density region gradually tends to smooth out.

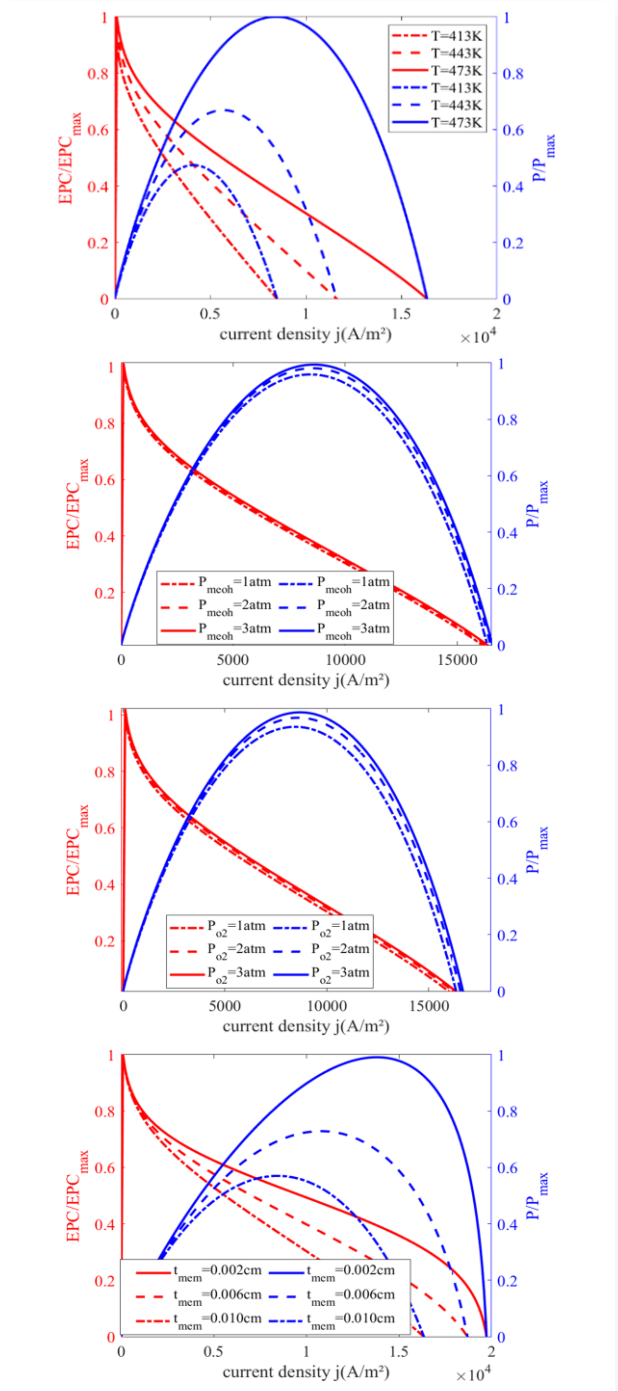

Fig. 5. The relationship between η and dimensionless EPC, P, η_{ex}.

It can also be seen from Fig. 5 that increasing the inlet pressure can improve $\overline{P}$ and $\overline{\mathrm{EPC}}$ of DMFC, but the improvement from the inlet pressure is not obvious. Increasing the inlet pressure can increase the supply rate of reactants, and the concentration gradient of the reactants involved in the reaction and supply is reduced, so that the concentration loss is reduced, and the power dissipation becomes smaller and $\overline{P}$ increases. Increasing the inlet pressure also improves the mass transfer of the reactants at both poles, expelling the water vapor generated at the cathode more easily, taking away more heat, reducing irreversible exergy loss, and improving the $\overline{\mathrm{EPC}}$.

Figure 6 reflects the power density of DMFC and the variation of EPC with the inlet pressure at different operating temperatures. It is obvious that the maximum power density of DMFC constantly increases with the increase of inlet gas. Since the exchange current density increases with the increase of operating pressure, the activation polarization loss will decrease and the reversible potential will increase. Therefore, as the operating pressure increases, the irreversible loss of DMFC decreases and the maximum power density of DMFC increases accordingly. Numerically, when the operating temperature is 453 K and the operating temperature of DMFC increases from 1 atm to 3 atm, the maximum power density of DMFC increases from 1563 W/m^2 to 1689 W/m^2, an improvement of only 8%, and EPC increases from 0.3344 to 0.3528, an improvement of 5.5%. Numerical analysis shows that the increase in operating pressure does not improve the DMFC performance as significantly as the increase in operating temperature. In addition, increasing the operating pressure requires additional power consumption to compress the inlet reactants.

Figure 7 reflects the power density of DMFC and the variation of EPC with operating temperature at different inlet air. It can be seen from the figure that the maximum power density of DMFC becomes larger as the operating temperature increases. This is due to the fact that the increase in the operating temperature leads to an increase in the exchange current density and hence the activation overpotential decreases with the increase in the exchange current density. At the same time, the increase in the operating temperature increases the proton conductivity and thus decreases the ohmic overpotential of DMFC. As a result, the power loss from ohmic overpotential and activation overpotential will be reduced. When the inlet pressure is 1 atm and the operating temperature is 413 K, the corresponding maximum power density is 371 W/m^2, and when the operating temperature increases to 473 K, the corresponding maximum power density reaches 1833 W/m^2, which indicates that when the operating temperature of DMFC increases from 413 K to 473 K, the maximum power density of the DMFC increases by 4.94 times. The results show that DMFC can significantly increase its maximum power density by choosing the right operating temperature range.

The DMFC operating parameter variation range is show in Table 2.

Table 2. DMFC operating parameter variation range.

Parameter	Value
Operating temperature, T_0 (K)	413-473
Electrolyte thickness, l_{mem} (cm)	0.0005-0.0015
Intake pressure P_{O_2}, P_{meoh} (atm)	1-5

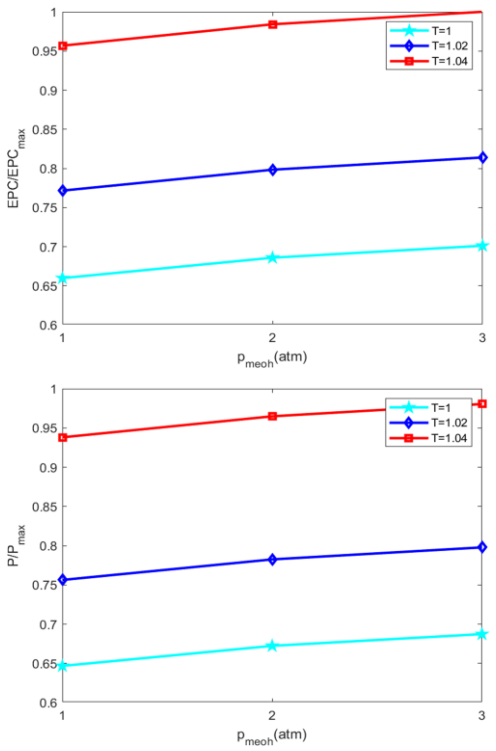

Fig. 6. $\overline{EPC}$ and $\overline{P}$ variation with the operating pressure.

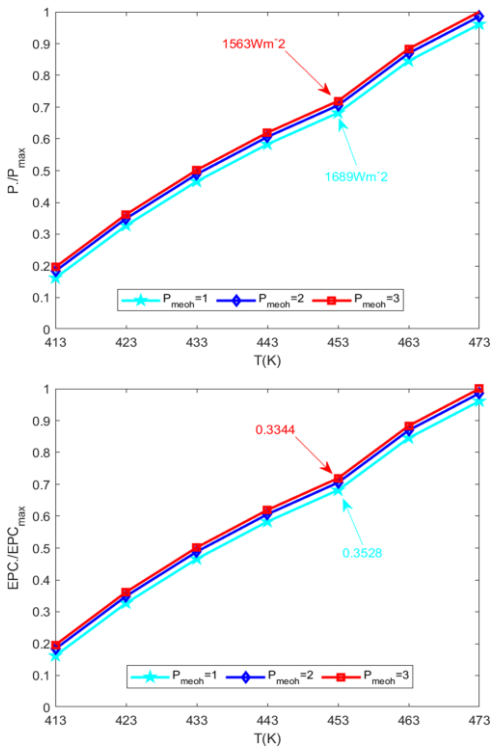

Fig. 7. $\overline{EPC}$ and $\overline{P}$ variation with the operating pressure.

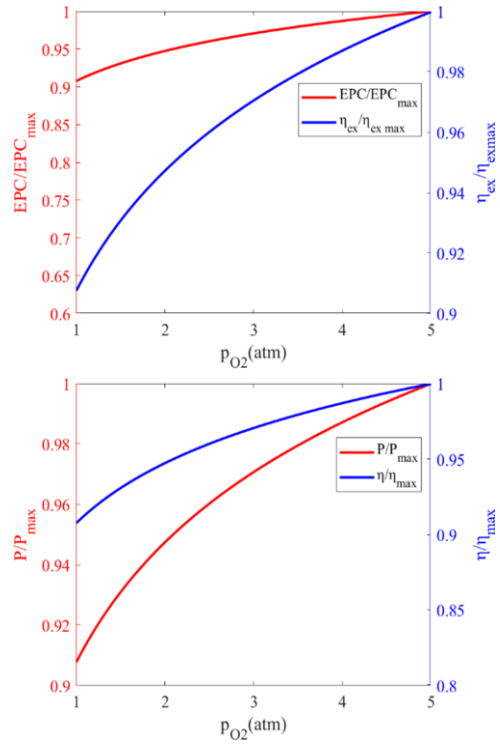

Fig. 8. The effect of inlet pressure P_{O_2} on the performance of DMFC.

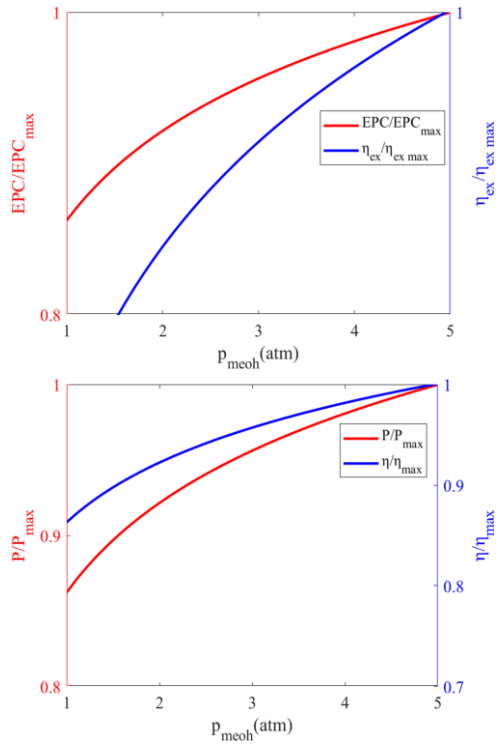

Fig. 9. The effect of inlet pressure P_{meoh} on the performance of DMFC.

Another factor that affects the performance of DMFC is the inlet pressure. On the one hand, increasing the inlet pressure accelerates the diffusion of reactant gases and improves the conditions for the mass transfer process between methanol and oxygen. In addition, it increases the concentration of reactants and reduces the effect of concentration polarization on the reversible potential. Figures 8 and 9 represent the effect of oxygen and methanol inlet pressures on DMFC performance, respectively.

From the figures, it can be seen that the power density and efficiency of DMFC increases with the increase of methanol and oxygen inlet pressures. The increase in power density and effi-

ciency in numerical value is not significant when the oxygen inlet pressure increases from 1 atm to 5 atm, but the value of power density increases significantly when the methanol inlet pressure increases from 1 atm to 5 atm, and the efficiency also increases at the same time. The power density and efficiency curves gradually decrease with the increase of methanol pressure because when the methanol concentration is too high, the rate of increase of reversible potential loss due to the concentration polarization is higher than the rate of decrease of reversible potential loss due to the increase of methanol pressure, so the power density and efficiency performance curves gradually smooth out.

Figure 10 reflects the effect of membrane thickness on DMFC power density, efficiency, exergy efficiency and EPC. It can be seen from the figure that the power density, efficiency and exergy efficiency and EPC all increase with decreasing membrane thickness, which is mainly due to the fact that decreasing proton membrane thickness will make the path length between the ions crossing from the anode to the cathode shorter, resulting in a lower ohmic potential of DMFC. However, if the proton membrane is too thin, it will lead to the penetration of methanol fuel from the anode to the cathode through the concentration difference, and cause problems such as short circuit and proton membrane rupture. Therefore, choosing the right proton membrane is crucial to enhance the performance of DMFC.

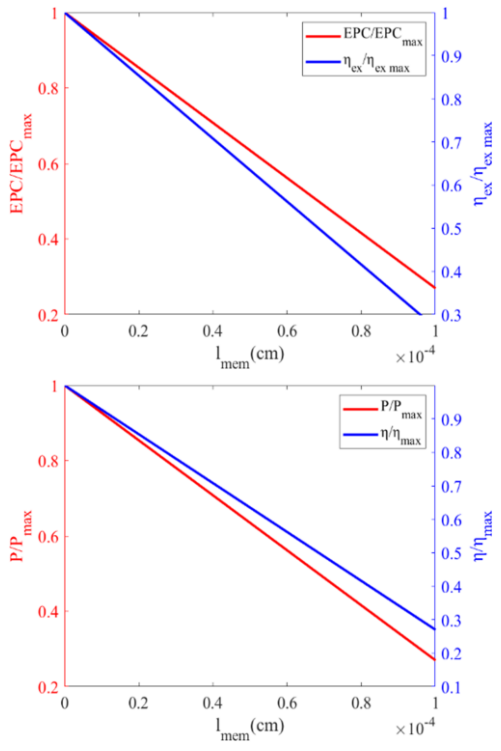

Fig. 10. Effect of membrane thickness on DMFC performance.

Figure 11 shows the relationship between EPC and efficiency before and after optimization of DMFC parameters. It can be seen that the EPC increases with increasing inlet pressure when the set membrane thickness l_{mem} and efficiency η are the same, increasing the inlet pressure can significantly improve the EPC of DMFC, indicating that the operating pressure has an effect on the power density and exergy destruction rate. When the operating pressure is the same, the efficiency of DMFC can be improved by improving the membrane thickness. By increasing the operating pressure and reducing the membrane thickness, the efficiency and EPC of DMFC will be significantly improved, which not only reduces the fuel consumption but also the heat loss in energy. However, if the thickness of the membrane is too low, methanol will come to the cathode side through the proton membrane more easily, which aggravates the methanol crossover phenomenon, thus accelerating the corrosion of DMFC and reducing the service life of DMFC.

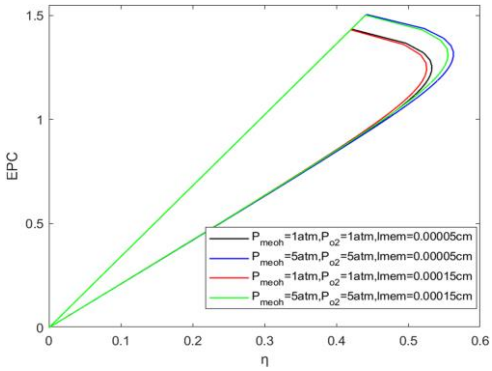

Fig. 11. Exergetic performance coefficient versus energy efficiency.

In addition, when higher pressure is provided to the inlet, extra power is consumed to compress the inlet reactant. In practice, when DMFC is applied to vehicles, the EPC and efficiency of DMFC can be improved by increasing the inlet pressure and reducing the membrane thickness.

4. Conclusions

In order to evaluate the thermodynamic performance of DMFC, the finite-time thermodynamic method is used to model DMFC considering three overpotentials and a new criterion, and exergy performance factor, the ratio of power to exergy loss rate are proposed to analyze the performance of DMFC. Relationships between EPC, power density, exergy efficiency and energy efficiency are obtained, and the results show that EPC can replace power density as a new performance metric. In the analysis of DMFC model, the effect of different parameters on power density, efficiency, exergy efficiency and EPC is analyzed. Analysis of the data reveals that EPC has the same trend as energy efficiency but represents different specific meanings. EPC_{max} stands for the fact that DMFC has the highest external output while minimizing the dissipation in the environment. Therefore, the higher the EPC_{max} of DMFC, the better the performance in terms of energy and ecology. In addition, increasing the inlet pressure and decreasing the film thickness can significantly improve the energy efficiency. This new criterion can be used in the future engineering field to analyze fuel cell vehicles.

Acknowledgement

We gratefully acknowledge the financial support of the Scientific Research Foundation of Nanjing Forestry University (No. GXL2018004).

References

[1] Mallick, R.K., Thombre, S.B., & Shrivastava, N.K. (2015). A critical review of the current collector for passive direct methanol fuel cells. *Journal of Power Sources*, 285, 510–529. doi: 10.1016/j.jpowsour.2015.03.089

[2] Kamarudin, S.K., Achmad, F., & Daud, W.R.W. (2009). Overview on the application of direct methanol fuel cell (DMFC) for portable electronic devices. *International Journal of Hydrogen Energy*, 34(16), 6902–6916. doi: 10.1016/j.ijhydene.2009.06.013

[3] Kimiaie, N., Wedlich, K., Hehemann, M., Lambertz, R., Mueller, M., Korte, C., & Stolten, D. (2014). Results of a 20 000 h lifetime test of a 7 kW direct methanol fuel cell (DMFC) hybrid system - Degradation of the DMFC stack and the energy storage. *Energy & Environmental Science*, *7*(9), 3013–3025. doi: 10.1039/C4EE00749B

[4] Karaoglan, M.U., Ince, A.C., Colpan, C.O., & Selman, J.R. (2019). Simulation of a hybrid vehicle powertrain having direct methanol fuel cell system through a semi-theoretical approach. *International Journal of Hydrogen Energy*, 44(34), 18981−18992. doi: 10.1016/j.ijhydene.2018.11.039]

[5] Yildirim, M.H., Schwarz, A., Stamatialis, D.F., & Wessling, M. (2009). Impregnated membranes for direct methanol fuel cells at high methanol concentrations. *Journal of Membrane Science*, 328, 127–133. doi: 10.1016/j.memsci.2008.11.051

[6] Li, Z., Hao, X., Cheng, G., Huang, S., Han, D., Xiao, M., Wang, S., & Meng, Y. (2021). In situ implantation of cross-linked functional POSS blocks in Nafion® for high performance direct methanol fuel cells. *Journal of Membrane Science*, 640(119798), 119798. doi: 10.1016/j.memsci.2021.119798.

[7] Huang, H.H., Ma, Y.F., Jiang, Z.Q., & Jiang, Z.J. (2021). Spindle-like MOFs-derived porous carbon filled sulfonated poly (ether ether ketone): A high performance proton exchange membrane for direct methanol fuel cells. *Journal of Membrane Science*, 636(119585). doi: 10.1016/j.memsci.2021.119585

[8] Yogarathinam, L.T., Jaafar, J., Ismail, A.F., Goh, P.S., Gangasalam, A., Hanifah, M.F.R., Wong, K.C., Subramaniam, M.N., & Peter, J. (2021). Functionalized boron nitride embedded sulfonated poly (ether ether ketone) proton exchange membrane for direct methanol fuel cell applications. *Journal of Environmental Chemical Engineering*, 9(5), 105876. doi: 10.1016/j.jece.2021.105876

[9] Yuan, W., Hou, C., Wu, J., Zhang, Y., & Zhang, X. (2023). A direct methanol fuel cell with outstanding performance via capillary distillation. *Chemical Engineering Journal (Lausanne, Switzerland: 1996)*, 470(143663), 143663. doi: 10.1016/j.cej.2023.143663.

[10] Mathew, A.S., Naigil, B., George, E., Benny, E., & Baby, R. (2022). Design, fabrication and testing of a direct methanol fuel cell stack. *Journal: Materials Today: Proceedings*, 58(1), 400–406. *International Conference on Artificial Intelligence and Energy Systems*, 12–13 June, 2021, Jaipur, India. doi: 10.1016/j.matpr.2022.02.338

[11] Li, X., He, Y., Yin, B., Miao, Z., & Li, X. (2008). Exergy flow and energy utilization of direct methanol fuel cells based on a mathematic model. *Journal of Power Sources*, 178(1), 344–352. doi: 10.1016/j.jpowsour.2007.08.019

[12] Hotz, N., Lee, M.T., Grigoropoulos, C.P., Senn, S.M. & Poulikakos, D. (2006). Exergetic analysis of fuel cell micropowerplants fed by methanol. *International Journal of Heat and Mass Transfer*, 49(15–16), 2397–2411. doi: 10.1016/j.ijheatmasstransfer.2006.03.007

[13] Yang, Q.-W., Hu, X.-Q., Lei, X.-C., Zhu, Y., Wang, X.-Y., & Ji, S.-C. (2018). Adaptive operation strategy for voltage stability enhancement in active DMFCs. *Energy Conversion and Management*, 168, 11–20. doi: 10.1016/j.enconman.2018.04.110

[14] Liu, G., Qin, Y., Yin, Y., Bian, X., & Kuang, C. (2020). Thermodynamic modeling and exergy analysis of proton exchange membrane fuel cell power system. *International Journal of Hydrogen Energy*, 45(54), 29799–29811. doi: 10.1016/j.ijhydene.2019.08.203

[15] Li, C., Liu, Y., Xu, B., & Ma., Z. (2019). Finite time thermodynamic optimization of an irreversible proton exchange membrane fuel cell for vehicle use. *Processes*, 7(7), 419. doi: 10.3390/pr7070419

[16] Chen, Y.Z., Zhao, D.D., Xu, J.Z., Wang, J., & Lund, P.D. (2021). Performance analysis and exergo-economic optimization of a solar-driven adjustable tri-generation system. *Energy Conversion and Management*, 233, 113873. doi: 10.1016/j.enconman.2021.113873

[17] Qi, C.Z., Du, Y.X., Chen, L.E., Yin, Y., & Ge, Y.L. (2023). Modeling and thermodynamic optimization of a solar-driven two-stage multi-element thermoelectric generator. *Journal of Cleaner Production*, 418, 138147. doi: 10.1016/j.jclepro.2023.138147

[18] Qi, C.Z., Chen, L.E., Ge, Y.L., Feng, H., & He, Z.(2022). Heat transfer effect on the performance of thermal Brownian heat engine. *Energy Reports*, 8, 3002−3010. doi: 10.1016/j.egyr.2022.02.063

[19] Bahrami, H., & Faghri, A. (2011). Exergy analysis of a passive direct methanol fuel cell. *Journal of Power Sources*, 196(3), 1191−1204. doi: 10.1016/j.jpowsour.2010.08.087

[20] Ishihara, A., Mitsushima, S., Kamiya, N., & Ota, K. (2004). Exergy analysis of polymer electrolyte fuel cell systems using methanol. *Journal of Power Sources*, 126(1−2), 34−40. doi: 10.1016/j.jpowsour.2003.08.029

[21] Mert, S.O., & Özçelik, Z. (2013). Multi-objective optimization of a direct methanol fuel cell system using a genetic-based algorithm. *International Journal of Energy Research*, 37(10), 1256−1264. doi: 10.1002/er.2963

[22] Li, D., Li, S., Ma, Z., Xu, B., Lu, Z., Li, Y., & Zheng, M. (2021). Ecological performance optimization of a high temperature proton exchange membrane fuel cell. *Mathematics*, 9(12), 1378. doi: 10.3390/math9121332

[23] Li, C., Xu, B., & Ma, Z. (2020). Ecological performance of an irreversible proton exchange membrane fuel cell. *Science of Advanced Materials*, 12(8), 1225–1235. doi: 10.1166/sam.2020.3846

[24] Akkaya, A.V., Sahin, B., & Erdem, H.H. (2007). Exergetic performance coefficient analysis of a simple fuel cell system. *International Journal of Hydrogen Energy*, 32(17), 4600–4609. doi: 10.1016/j.ijhydene.2007.03.038

[25] Rosenthal, N.S., Vilekar, S.A., & Datta, R. (2012). A comprehensive yet comprehensible analytical model for the direct methanol fuel cell. *Journal of Power Sources*, 206, 129–143. doi: 10.1016/j.jpowsour.2012.01.080

[26] Bahrami, H., & Faghri, A. (2013). Review and advances of direct methanol fuel cells: Part II: Modeling and numerical simulation. *Journal of Power Sources*, 230, 303–320. doi: 10.1016/j.jpowsour.2012.12.009

[27] Lee, W.-Y., Kim, M., Sohn, Y.-J., & Kim, S.-G. (2016). Power optimization of a combined power system consisting of a high-temperature polymer electrolyte fuel cell and an organic Rankine cycle system. *Energy*, 113, 1062–1070. doi: 10.1016/j.energy.2016.07.093

[28] Guo, X., Zhang, H., Yuan, J., Wang, J., Zhao, J., Wang, F., Miao, H., & Hou, S. (2019). Energetic and exergetic analyses of a combined system consisting of a high-temperature polymer electrolyte membrane fuel cell and a thermoelectric generator with Thomson effect. *International Journal of Hydrogen Energy*, 44(31), 16918–16932. doi: 10.1016/j.ijhydene.2019.04.215

[29] Taner, T. (2018). Energy and exergy analyze of PEM fuel cell: A case study of modeling and simulations. *Energy*, 143, 284–294. doi: 10.1016/j.energy.2017.10.102

[30] Cohce, M.K., Dincer, I., & Rosen, M.A. (2011). Energy and exergy analyses of a biomass-based hydrogen production system. *Bioresource Technology*, 102(18), 8466–8474. doi: 10.1016/j.biortech.2011.06.020

[31] Obara, S., Tanno, I., Kito, S., Araki, M., & Sazaki, S. (2008). Exergy analysis of the woody biomass Stirling engine and PEM-FC combined system with exhaust heat reforming. *International Journal of Hydrogen Energy*, 33(9), 2289–2299. doi: 10.1016/j.ijhydene.2008.02.035

[32] Dincer, I., Hussain, M.M., & Al-Zaharnah, I. (2005). Energy and exergy utilization in the agricultural sector of Saudi Arabia. *Energy Policy*, 33(11), 1461–1467. doi: 10.1016/j.enpol.2004.01.004

[33] Sharifi, S., Rahimi, R., Mohebbi-Kalhori, D., & Çolpan, C. Ö. (2020). Coupled computational fluid dynamics-response surface methodology to optimize direct methanol fuel cell performance for greener energy generation. *Energy*, 198, 117293. doi: 10.1016/j.energy.2020.117293